

1 International Journal of Biomathematics
 2 Vol. 4, No. 3 (September 2011) 1–20
 3 © World Scientific Publishing Company
 4 DOI: 10.1142/S1793524511001234



5 **NOISE AND SEASONAL EFFECTS ON THE**
 6 **DYNAMICS OF PLANT–HERBIVORE**
 7 **MODELS WITH MONOTONIC PLANT**
 8 **GROWTH FUNCTIONS**

9 YUN KANG
 10 *Applied Sciences and Mathematics*
 11 *Arizona State University*
 12 *Mesa, AZ 85212, USA*
 13 *yun.kang@asu.edu*

14 DIETER ARMBRUSTER
 15 *School of Mathematical and Statistical Sciences*
 16 *Arizona State University*
 17 *Tempe, AZ 85287-1804, USA*
 18 *armbruster@asu.edu*

19 Received 18 March 2010
 20 Revised 11 August 2010

21 We formulate general plant–herbivore interaction models with monotone plant growth
 22 functions (rates). We study the impact of monotone plant growth functions in general
 23 plant–herbivore models on their dynamics. Our study shows that all monotone plant
 24 growth models generate a unique interior equilibrium and they are uniform persistent
 25 under certain range of parameters values. However, if the attacking rate of herbivore is
 26 too small or the quantity of plant is not enough, then herbivore goes extinct. Moreover,
 27 these models lead to noise sensitive bursting which can be identified as a dynamical
 28 mechanism for almost periodic outbreaks of the herbivore infestation. Montone and
 29 non-monotone plant growth models are contrasted with respect to bistability and crises
 30 of chaotic attractors.

31 *Keywords:* Monotone growth models; uniformly persistent; Neimark–Sacker bifurcation;
 32 heteroclinic bifurcation; periodic infestations; bistability; noise bursting; crisis of chaos.

33 **1. Introduction**

34 Interactions between plants and herbivores have been studied by ecologists for many
 35 decades. One focus of research is the effects of herbivores on plant dynamics [5]. In
 36 contrast, there is strong ecological evidence indicating that the population dynamics
 37 of plants has an important effect on the plant–herbivore interactions. In this paper,
 38 we investigate how plants with different population dynamics contribute to the
 39 interactions. Models for plant growth vary strongly [6]: Table 1 lists eight discrete-
 40 time models of plant population growth. The first seven models are introduced in

2 *Y. Kang & D. Armbruster*

Table 1. Growth models of plant population density.

Model	$f(P)$	Number of parameters	$f(0)$	Equilibrium
1	$1 + q - \frac{qP}{K}$	2	$1 + q$	K
2	$e^{\ln(1+q)[1-\frac{P}{K}]}$	2	$1 + q$	K
3	$e^{\ln(1+q)[1-\ln(1+P)]}$	2	$1 + q$	K
4	$\frac{w}{1+cP}$	2	w	$\frac{w-1}{c}$
5	$\frac{w}{1+P^b}$	2	w	$(w-1)^{\frac{1}{b}}$
6	$\frac{w}{(1+P)^b}$	2	w	$w^{\frac{1}{b}} - 1$
7	$\frac{w}{1+cP^b}$	3	w	$\frac{w^{\frac{1}{b}}-1}{c}$
8	$\frac{wP^{b-1}}{1+P^b}$	2	0	Positive roots of $wP^{b-1} = 1 + P^b$

1 the paper by Law and Watkinson [21] without inter-specific competition. All models
 2 are seasonal (discrete) models of the form $P_{t+1} = P_t f(P_t)$, where P_t is the density
 3 of a plant in season t and $f(\cdot)$ the per capita growth rate. In the absence of intra-
 4 specific competition the latter is given by $f(0)$, i.e. $1 + q$ in models 1–3 and w in
 5 models 4–8. The equilibrium density of the plant is given by K . The parameter c is
 6 the space per plant at which interference with neighbors becomes appreciable [21].
 7 The interpretation of the power parameter b depends on the model. Generally, these
 8 models fall into two classes, depending on whether $Pf(P)$ is a monotone function
 9 of P or not. Models 1–3 are unimodal, i.e. they have a single hump. They lead
 10 to complicated dynamics including period doubling, period windows and chaos [9].
 11 Models 4–8 are monotone, leading to much simpler dynamics. Model 8 has a growth
 12 function of Holling type III [23].

Notice that model 2 is the well-known Ricker model [24] which is unimodal and usually written as

$$P_{t+1} = P_t e^{r(1-\frac{P_t}{K})} \quad (1.1)$$

while model 4 is the Beverton–Holt model [3] usually written as

$$P_{t+1} = \frac{KP_t}{e^{-r}K + P_t(1 - e^{-r})} \quad (1.2)$$

13 The dynamics of the Ricker model (1.1) has been well studied. It shows period-
 14 doubling, chaos and period windows. A plant–herbivore model with Ricker dynamics
 15 in plant has been studied in [16] (also see similar models in [1, 20]) showing many
 16 forms of complex dynamics.

17 There are fair amount of literatures on seasonal (discrete) multi-species interac-
 18 tion or stage structure models (e.g. [1, 7, 8, 15, 16, 20, 26, 27, 31]), among which a
 19 few studies are related to discrete prey–predator (or host–parasite) interaction mod-
 20 els (e.g. [15, 16, 20]). Tuda and Iwasa [31] developed scramble-type and contest-type
 21 models to examine an evolutionary shift in the mode of competition among the bean

1 weevils. Jang [15] studied a discrete-time Beverton–Holt stock recruitment model
 2 with Allee effects. Kang *et al.* [16] and Kon [20] studied a discrete plant–herbivore
 3 (or host–parasite) interaction model with Ricker dynamics as the growth function
 4 of plant (or host in Kon [20]). In this paper, we investigate the impact of general
 5 monotone plant growth models on the dynamics of plant–herbivore interaction. Our
 6 study is different from others and our results are new. We show that all monotone
 7 plant growth models generate a unique interior equilibrium (Theorem 4.3) and they
 8 are uniformly persistent (see related definitions in [28]) for certain range of param-
 9 eters values (Theorem 4.5). If the attacking rate of herbivore is too small or the
 10 quantity of plant is not enough, then herbivore goes extinct (Theorem 4.2). In addi-
 11 tion, our numerical simulations suggest that these models lead to noise sensitive
 12 bursting which can be identified as a dynamical mechanism for almost periodic
 13 outbreaks of the herbivore infestation.

14 The rest of paper is organized as follows. In Sec. 2 we define two classes of
 15 monotone dynamics of single plant species. In Sec. 3 we formulate general plant–
 16 herbivore models for the plant dynamics introduced in Sec. 2. In Sec. 4 we analyze
 17 the dynamic behavior of these two general models, e.g. the global stability of the
 18 boundary equilibrium and uniform persistence of these models. In Sec. 5 we apply
 19 the theoretical results from Sec. 4 to a Beverton–Holt model and a Holling type III
 20 model. The analysis and numerical simulations suggest that Beverton–Holt model
 21 goes through Neimark–Sacker bifurcation with unique periodic orbit for a certain
 22 set of parameters values; while Holling type III model goes through heteroclinic
 23 bifurcation for a certain set of parameters values. Our study also shows that noise
 24 is an important factor for outbreak of herbivore. Finally, we compare monotone
 25 plant growth models to unimodal and multimodal plant growth models regarding
 26 their influence of plant–herbivore dynamics.

27 2. Monotone Growth Dynamics for a Single Plant Species

28 Consider

$$29 \quad P_{t+1} = P_t f(r, P_t) = F(r, P_t), \quad t \geq 0. \quad (2.1)$$

30 where P_t is the density of biomass in plant at generation t ; $F(r, P_t)$ is the growth
 31 function of biomass density and $f(r, P_t)$ is the per capita growth rate of the biomass
 32 density. Without intra-specific competition, we have $f(r, 0) = r$, i.e. r is the maximal
 33 per capita growth rate of the plant. This simple formulation (2.1) can give rise to
 34 a great diversity of dynamical behavior, depending on the expression used for the
 35 growth function $f(r, \cdot)$ and the values given to the parameters of that function.
 36 Several different functions have been considered. See [4] for a partial list of models
 37 with per capita growth rates that decline with increasing population density:

$$38 \quad \frac{\partial f(r, P)}{\partial P} < 0, \quad P \geq 0. \quad (2.2)$$

4 Y. Kang & D. Armbruster

1 In biological terms, this means that the per capita growth rate $f(r, P)$ decreases
 2 due to negative density-dependent mechanism such as intra-specific competition
 3 between individuals within a population. For convenience, we use $F(P), f(P)$
 4 instead of $F(r, P), f(r, P)$ since r is a fixed parameter. The well-known proto-
 5 types of the model (2.1) under this biological assumption are the Beverton–Holt
 6 and Ricker models. The dynamics of Ricker model has been extensively studied
 7 (e.g. [16, 20, 24]). Here, we focus on the Beverton–Holt prototype, i.e. the dynam-
 8 ics of the plant is monotonically increasing,

$$9 \quad F'(P) = \frac{dF(P)}{dP} \geq 0, \quad P \geq 0. \quad (2.3)$$

10 We can characterize the growth models of a single plant with assumption **H1** or
 11 **H2** or both **H1** and **H2**:

12 **H1:** $F(0) = 0$, $F(P)|_{P>0} > 0$, $F'(P) > 0$ and $\lim_{P \rightarrow +\infty} F(P) = C > 0$.

13 **H2:** $f(P)|_{P \geq 0} \geq 0$, $f'(P) < 0$ and $\lim_{P \rightarrow +\infty} f(P) = 0$.

14 In the biological sense, **H1** implies that the population density in one year is a
 15 increasing function $F(P)$ of the density in the previous year and its per capita
 16 growth function $f(P)$ may be increasing or decreasing or both, which implies that
 17 plant suffers from the extremes of contest intra-specific competitive interaction (see
 18 [11]); **H2** implies that the per capita growth function of the plant is a decreasing
 19 function due to intra-specific competition and the population density of a plant can
 20 be an increasing or decreasing function or both with respect to its density, which
 21 implies that plant suffers from the extremes of scramble intra-specific competitive
 22 interactions (see [11]). In this paper, we study the population dynamics associated
 23 with plants that satisfy **H1** or **H2** or both **H1** and **H2**. The specific assumptions
 24 will be addressed in the models. The following proposition summarizes the dynamics
 25 of plant in the absence of herbivore.

26 **Proposition 2.1.** (1) Assume that **H1** holds and there are $n + 1$ consecutive,
 27 distinct and non-degenerate solutions $\bar{P}^i, i = 0, 1, \dots, n$ of $P = F(P)$ with the
 28 following property

$$29 \quad 0 = \bar{P}^0 < \bar{P}^1 < \dots < \bar{P}^n.$$

30 If \bar{P}^0 is stable (unstable) then the even \bar{P}^i are stable (unstable) while the odd
 31 \bar{P}^i are unstable (stable). In particular, \bar{P}^n is always stable. Moreover, define
 32 the map $P_{t+1} = F(P_t)$, then for any $\epsilon > 0$, there exists N large enough, such
 33 that for all $t > N$, we have

$$34 \quad P_{t+1} = F(P_t) \leq \bar{P}^n + \epsilon.$$

35 (2) Assume that **H2** holds, then $P = Pf(P)$ has at most two roots, i.e. $P = 0$ and
 36 the possible root of $1 = f(P)$.

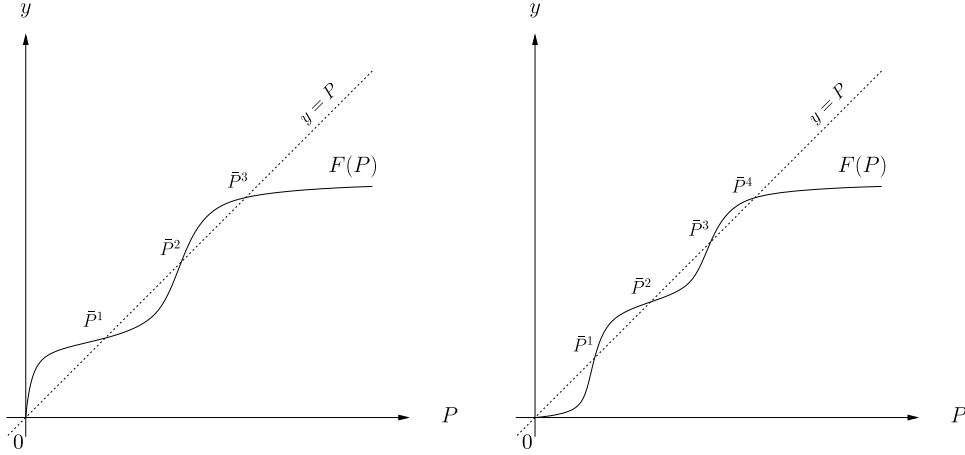


Fig. 1. Possible configurations of the staircase diagrams.

1 **Proof.** Possible configurations of the staircase diagrams of Fig. 1 show the alternating stable and unstable equilibria. If **H1** holds, then we have

2

3
$$0 < \lim_{P \rightarrow +\infty} F(P) = C < 1 \quad \text{and} \quad 0 < F'(\bar{P}^n) < 1.$$

4 This implies that the largest equilibrium \bar{P}^n is locally stable.

5 If an initial condition P_0 satisfies $P_0 \leq \bar{P}^n$, then **H1** implies that

6
$$P_1 = F(P_0) \leq F(\bar{P}^n) = \bar{P}^n$$

7 and by induction, $P_t \leq \bar{P}^n$ for all $t \geq 1$. In the case that the initial condition is larger than \bar{P}^n , i.e. $P_0 > \bar{P}^n$, then **H1** and the fact that \bar{P}^n is the largest positive root of $P = F(P)$ indicate that $F(P) < P$ for all $P > \bar{P}^n$. Thus, we have

8

9

10
$$\bar{P}^n = F(\bar{P}^n) \leq P_1 = F(P_0) < P_0.$$

11 Therefore, by induction, we know that the sequence $\{P_t\}_{t=0}^{\infty}$ is decreasing and converges to \bar{P}^n as $t \rightarrow \infty$. This indicates that for any $\epsilon > 0$, there exists N large enough, such that for all $t > N$, we have $P_{t+1} = F(P_t) \leq \bar{P}^n + \epsilon$. In other cases, we have $P_{t+1} = F(P_t) < \bar{P}^n$ for all $t > 0$.

12

13

14

15 Since $f(P)$ is a differentiable and strictly decreasing function of P , thus $1 = f(P)$ has at most one solution. Therefore, the statement holds. \square

16

17 **3. Plant–Herbivore Models**

18 Insect and plant survival rates often appear to be nonlinear functions of plant and insect density, respectively (see [5, 10]). In our discrete-time models, we therefore assume that the plant population growth is a nonlinear function of herbivore and plant density, and that plant population growth decreases gradually with increasing herbivore density. Similarly, we assume that the density of herbivore population

19

20

21

22

6 *Y. Kang & D. Armbruster*

1 depends on both the plant and herbivore's density rather than only the herbivore
 2 density [5]. A final key feature of many plant–herbivore interactions is that, in the
 3 absence of the herbivore, we have a monotone growth dynamics as discussed in the
 4 previous section.

Let P_t represent the density of edible plant biomass in generation t and H_t represent the population density of herbivore. The effect of the herbivore on the plant population growth rate is described by the function $g(a, H_t)$ with $g(a, 0) = 1$. Here the parameter a measures the damage caused by herbivore, e.g. feeding rate. We assume that the herbivore population density is proportional to a function of plant density $h(P_t)$ and a nonlinear function of herbivore density $l(H_t)$. Therefore, the structure of our models is

$$P_{t+1} = P_t f(P_t) g(a, H_t), \quad (3.1)$$

$$H_{t+1} = h(P_t) l(H_t). \quad (3.2)$$

5 Many consumer–resource models assume a nonlinear relationship between resource
 6 population size and attack rate (see [2, 30]). For plants and insect herbivores,
 7 we similarly expect a nonlinear functional relationship, due to herbivore foraging
 8 time and satiation. The relationship is expressed in terms of plant biomass units
 9 rather than population size, because herbivores are unlikely to kill entire plants
 10 (see [5, 10]).

Our model has the following features: without the herbivore, we assume a monotone growth rate, i.e. **H1** holds. The growth function $F(P_t)$ determines the amount of new leaves available for consumption for the herbivore in generation t . We assume that the herbivores search for plants randomly. The area consumed is measured by the parameter a , i.e. a is a constant that correlates to the total amount of the biomass that an herbivore consumes. The herbivore has a one year life cycle, the larger a , the faster the feeding rate. After attacks by herbivores, the biomass in the plant population is reduced to

$$P_{t+1} = P_t f(P_t) e^{-aH_t}, \quad (3.3)$$

where $g(a, H_t)$ in (3.1) is defined as

$$g(a, H_t) = e^{-aH_t}. \quad (3.4)$$

The term $h(P_t)$ in (3.2) describes how the biomass in the plants is converted to the biomass of the herbivore. It differs depending on the relative timing of herbivore feeding and growth. If the herbivore attacks the plant before the plant grows, then we have $h(P_t) = P_t$, otherwise, $h(P_t) = P_t f(P_t)$. Since the biomass of herbivore comes from whatever they eat, $h(P_t)$ is the available biomass of a plant that can be converted into the herbivore's biomass. The term $l(H_t)$ describes the fraction of $h(P_t)$ that can be used by the herbivore, i.e. $l(H_t) = 1 - e^{-aH_t}$. Therefore, the evolution of the plant–herbivore system is either described by **Model I**:

$$P_{t+1} = F(P_t) e^{-aH_t}, \quad (3.5)$$

$$H_{t+1} = P_t [1 - e^{-aH_t}], \quad (3.6)$$

describing the dynamics of a system where the plant is attacked before it has a chance to grow while **Model II**:

$$P_{t+1} = F(P_t)e^{-aH_t}, \quad (3.7)$$

$$H_{t+1} = F(P_t)[1 - e^{-aH_t}] \quad (3.8)$$

1 describes the dynamics when the plant grows first before being attacked.

2 4. Mathematical Analysis

3 First, we can easily see that \mathbb{R}_+^2 is positively invariant for both Models I and II. In
4 addition, we have the following lemma.

5 **Lemma 4.1.** *If **H1** holds, then $\limsup_{t \rightarrow \infty} \max\{P_t, H_t\} \leq \bar{P}^n$ for both Models I
6 and II.*

7 **Proof.** For Model I,

$$8 \quad H_{t+1} = P_t[1 - e^{-aH_t}] \leq P_t$$

9 and for Model II,

$$10 \quad H_{t+1} = P_t f(P_t)[1 - e^{-aH_t}] \leq F(P_t).$$

11 Since condition **H1** holds for $F(P)$, then from Proposition 2.1, we can conclude that
12 for any $\epsilon > 0$, there exists N large enough, such that for all $t > N$, the following
13 holds

$$14 \quad P_{t+1} = F(P_t)e^{-aH_t} \leq F(P_t) \leq \bar{P}^n + \epsilon.$$

15 Therefore, we have $\limsup_{t \rightarrow \infty} \max\{P_t, H_t\} \leq \bar{P}^n$ for both Models I and II. \square

16 4.1. Equilibria and their stability

17 If, in the absence of the herbivore, there exist $n + 1$ equilibria of the plant dynamics,
18 then both Models I and II have $n + 1$ boundary equilibria of the form

$$19 \quad E_{00} = (0, 0) \quad \text{and} \quad E_{i0} = (\bar{P}^i, 0), \quad i = 1, 2, \dots, n.$$

20 Their local stability can be determined by the eigenvalues of their Jacobian
21 matrices.

22 It is easy to check that the Jacobian matrices of Models I and II are identical
23 at these boundary equilibria: the eigenvalues of their associated Jacobian matrix at
24 $(0, 0)$ are $F'(0)$ and 0; the eigenvalues of their associated Jacobian matrix at $(\bar{P}^i, 0)$
25 are $F'(\bar{P}^i)$ and $a\bar{P}^i$. The following theorems summarize the global dynamics:

26 **Theorem 4.2.** *Assume that **H1** holds for both Models I and II. If $F'(0) < 1$ and
27 $(0, 0)$ is the only boundary equilibrium, then Models I and II are globally stable at
28 $(\bar{P}^0, 0) = (0, 0)$. More generally, if $a\bar{P}^n < 1, n \in \mathbb{Z}_+$, then $\lim_{t \rightarrow \infty} H_t = 0$ for both
29 Models I and II.*

8 *Y. Kang & D. Armbruster*

Proof. From Lemma 4.1, we know that for any $\epsilon > 0$, there exists N large enough, such that for all $t > N$, we have

$$P_{t+1} = F(P_t)e^{-aH_t} \leq F(P_t) \leq \bar{P}^n + \epsilon \quad (4.1)$$

1 Since $a\bar{P}^n < 1$, then for ϵ small enough, we have

$$2 \quad aP_t \leq a(\bar{P}^n + \epsilon) < 1 \quad \text{and} \quad aF(P_t) \leq a(\bar{P}^n + \epsilon) < 1 \quad \text{for all } t \geq N.$$

Thus, for Model I,

$$H_{t+1} = P_t[1 - e^{-aH_t}] = H_t P_t \frac{[1 - e^{-aH_t}]}{H_t} \leq aH_t P_t \leq a(\bar{P}^n + \epsilon)H_t \quad (4.2)$$

and for Model II,

$$H_{t+1} = F(P_t)H_t \frac{[1 - e^{-aH_t}]}{H_t} \leq aH_t F(P_t) \leq a(\bar{P}^n + \epsilon)H_t. \quad (4.3)$$

3 Therefore, we have $H_t \leq [a(\bar{P}^n + \epsilon)]^{t-N} H_N$, for all $t > N$. This indicates that
 4 $\lim_{t \rightarrow \infty} H_t = 0$ for both Models I and II. Hence solutions of Models I and II are
 5 globally attracted to the boundary dynamics. \square

6 Theorem 4.2 indicates that herbivore cannot maintain its population if its
 7 attracting rate is too small or there is not enough food, i.e. $a\bar{P}^n < 1$. In addition,
 8 the special case of Theorem 4.2 when $n = 1$ leads to the following remarks.

9 **Remark.** Assume that the hypotheses of Theorem 4.2 hold. If $n = 1$, then from
 10 Proposition 2.1, we have

- 11 (1) If $F'(0) < 1$, then \bar{P}^1 is a source;
 12 (2) If $F'(0) > 1$, then \bar{P}^1 is a sink.

13 Hence, if $F'(0) > 1$ and $n = 1$, then $(\bar{P}^1, 0)$ attracts all non-trivial solutions.

14 4.2. *Unique interior equilibrium*

15 Interior equilibria are determined by the intersections of the nullclines. Notice that
 16 if **H1** holds, then $y = F(P)$ is a differentiable and monotone function of P and
 17 maps \mathbb{R}^+ to $[0, C)$. Its inverse exists and can be written as $P = F^{-1}(y)$ which
 18 maps $[0, C)$ to \mathbb{R}^+ . Similarly, if **H2** holds, then $y = f(P)$ is a differentiable and
 19 monotone function of P and maps \mathbb{R}^+ to $[0, M)$. Its inverse exists and can be written
 20 as $P = f^{-1}(y)$ which maps $[0, M)$ to \mathbb{R}^+ . Here $C = F(\infty)$ and $M = f(0)$ are some
 21 positive constants. If (\bar{P}, \bar{H}) is an interior equilibrium, then it is the solution of the
 22 two equations:

(1) For Model I,

$$P = f^{-1}(e^{aH}), \quad (4.4)$$

$$P = \frac{H}{1 - e^{-aH}}. \quad (4.5)$$

(2) For Model II,

$$P = \frac{H}{e^{aH} - 1}, \quad (4.6)$$

$$P = F^{-1}\left(\frac{H}{1 - e^{-aH}}\right). \quad (4.7)$$

1 If $F(P)$ is monotonically increasing, i.e. **H1** holds, then $F^{-1}\left(\frac{H}{1 - e^{-aH}}\right)$ is an increasing
2 function of H which attains its minimum at $H = 0$, i.e.

$$3 \quad \min_{H \geq 0} \left\{ F^{-1}\left(\frac{H}{1 - e^{-aH}}\right) \right\} = F^{-1}\left(\frac{H}{1 - e^{-aH}}\right) \Big|_{H=0} = F^{-1}\left(\frac{1}{a}\right).$$

4 Similarly, if $f(P)$ is monotonically decreasing, i.e. **H2** holds, then $f^{-1}(e^{aH})$ is a
5 decreasing function of H which attains its maximum at $H = 0$, i.e.

$$6 \quad \max_{H \geq 0} \{f^{-1}(e^{-aH})\} = f^{-1}(e^{-aH}) \Big|_{H=0} = f^{-1}(0).$$

7 **Theorem 4.3.** (a) Assume that both **H1** and **H2** hold for Model I, then Model I
8 has at most one interior equilibrium which occurs when $f^{-1}(0) > \frac{1}{a}$. The interior
9 equilibrium emerges generically through a transcritical bifurcation from the
10 largest boundary equilibrium \bar{P}^n when $\bar{P}^n = \frac{1}{a}$, where $n \geq 1$.
11 (b) Assume that **H1** holds for Model II, then Model II has at most one interior
12 equilibrium which occurs when $F^{-1}\left(\frac{1}{a}\right) < \frac{1}{a}$. The interior equilibrium
13 emerges generically through a transcritical bifurcation from the largest boundary
14 equilibrium \bar{P}^n when $\bar{P}^n = \frac{1}{a}$, where $n \geq 1$.

15 **Proof.** The proofs for (a) and (b) are similar. We show case (b): the interior
16 equilibria of Model II are determined by the intersections of the nullclines (4.6) and
17 (4.7). Since (4.6) is a decreasing function and (4.7) is an increasing function, they
18 have only one interior intersection if the following inequality holds

$$19 \quad \min_{H \geq 0} \left\{ F^{-1}\left(\frac{H}{1 - e^{-aH}}\right) \right\} < \max_{H \geq 0} \left\{ \frac{H}{e^{aH} - 1} \right\} \Rightarrow F^{-1}\left(\frac{1}{a}\right) < \frac{1}{a}.$$

The Jacobian matrix of Model II evaluated at the boundary equilibrium
($\bar{P}^i, 0$) is

$$J|_{(\bar{P}^i, 0)} = \begin{bmatrix} F'(\bar{P}^i) & -a\bar{P}^i \\ 0 & a\bar{P}^i \end{bmatrix} \quad (4.8)$$

20 with its eigenvalues as $\lambda_1 = a\bar{P}^i$ and $\lambda_2 = F'(\bar{P}^i)$. Thus, at the largest boundary
21 equilibrium ($\bar{P}^n, 0$), we have

- 22 (1) $\lambda_1|_{(\bar{P}^n, 0)} = a\bar{P}^n$ and $\lambda_2|_{(\bar{P}^n, 0)} = F'(\bar{P}^n) < 1$;
23 (2) $\frac{\partial \lambda_1}{\partial a}|_{(\bar{P}^n, 0)} = \bar{P}^n$ and $\frac{\partial \lambda_2}{\partial a}|_{(\bar{P}^n, 0)} = 0$.

10 Y. Kang & D. Armbruster

1 In the case that $\bar{P}^n = \frac{1}{a}$, we have $\lambda_1|_{(\bar{P}^i, 0)} = a\bar{P}^i < 1, i = 1, \dots, n-1$ and

$$2 \quad \lambda_2|_{(\bar{P}^n, 0)} = a\bar{P}^n < \lambda_1|_{(\bar{P}^n, 0)} = 1 \quad \text{and} \quad \frac{\partial \lambda_1}{\partial a} \Big|_{(\bar{P}^n, 0)} = \bar{P}^n = \frac{1}{a} > 0.$$

The eigenvector associated with the eigenvalue $\lambda_1|_{(\bar{P}^n, 0)} = a\bar{P}^n$ is

$$3 \quad V|_{\lambda_1 = a\bar{P}^n} = \begin{bmatrix} -\frac{a\bar{P}^n - F'(\bar{P}^n)}{a\bar{P}^n} x_2 \\ x_2 \end{bmatrix}. \quad (4.9)$$

4 If $a\bar{P}^n = 1$, then the two components of (4.9) have opposite signs. This implies
5 that by choosing $x_2 > 0$, the unstable manifold of E_{n0} points toward the interior of
6 X_{11} . Therefore, apply Theorem 13.5 in the book by Smoller [29], the unique interior
7 equilibrium of Model II emerges generically through a transcritical bifurcation from
the largest boundary equilibrium \bar{P}^n when $\bar{P}^n = \frac{1}{a}$, where $n \geq 1$. \square

8 4.3. Uniform persistence of Models I and II

We define the sets

$$X = \{(P, H) : P \geq 0, H \geq 0\},$$

$$X_{11} = \{(P, H) \in X : PH > 0\},$$

$$\partial X_{11} = X \setminus X_{11}$$

9 and consider the additional hypothesis:

10 **H3:** The smallest positive root \bar{P}^1 of $P = F(P) = Pf(P)$ satisfies $a\bar{P}^1 > 1$, and
11 in addition, $f(0) > 1$.

12 In the following, we show that Models I and II are uniformly persistent with respect
13 to $(X_{11}, \partial X_{11})$ if both **H1** and **H3** hold, i.e. for any initial condition $(P_0, H_0) \in X_{11}$,
14 there exists some $\epsilon > 0$ such that $\liminf_{t \rightarrow \infty} \min\{P_t, H_t\} \geq \epsilon$.

15 **Lemma 4.4.** X_{11} and ∂X_{11} are positively invariant for (3.5)–(3.6) and (3.7)–(3.8).

16 The following theorem is the main result of this subsection.

17 **Theorem 4.5.** If $a\bar{P}_1 > 1$, then (3.5)–(3.6) and (3.7)–(3.8) are uniformly persistent
18 with respect to $(X_{11}, \partial X_{11})$ provided that they satisfy both **H1** and **H3**.

19 **Proof.** From Lemma 4.4 and Proposition 4.1, we obtain that the systems (3.5)–
20 (3.6) and (3.7)–(3.8) are point dissipative. This combined with the fact that the
21 semiflow generated by these systems is asymptotically smooth (this is automatic,
22 since the state space is in \mathbb{R}_+^2), gives the existence of the compact attractors of
23 points for both systems (see [28]).

24 Notice that the omega limit set of $S_1 = \{(P, H) \in \mathbb{R}_+^2 : P = 0\}$ is the trivial
25 boundary equilibrium E_{00} . Let $L(P, H) = P$ be an average Lyapunov function,

1 then we have $L(P, H)|_{S_1} = 0$. Since the system satisfies **H3**, then the following
2 inequality holds

$$3 \quad \sup_{t \geq 0} \liminf_{(P_0, H_0) \rightarrow (0, 0)} \frac{P_t}{P_0} = \sup_{t \geq 0} \liminf_{(P_0, H_0) \rightarrow (0, 0)} \prod_{j=0}^{t-1} f(P_j) e^{-aH_j} = \sup_{t \geq 0} (f(0))^t > 1,$$

4 where $(P_0, H_0) \in X \setminus S_1$. Therefore, by applying Theorem 2.2 in [14] and its corol-
5 lary to the systems (3.5)–(3.6) and (3.7)–(3.8), we obtain persistence of the plant
6 population, i.e. for any initial condition $P_0 > 0$, we have $\liminf_{t \rightarrow \infty} P_t \geq \epsilon$.

7 The fact that the plant population is uniformly persistent implies that the sys-
8 tem (3.5)–(3.6) or (3.7)–(3.8) can be restricted in $X \cap \{(P, H) \in \mathbb{R}_+^2 : P \geq \epsilon\}$.
9 According to Proposition 2.1, we can conclude that the omega limit sets of
10 $S_2 = \{(P, H) \in \partial X_{11} : P > 0\}$ are $\{E_{i0}, 1 \leq i \leq n\}$. Since $a\bar{P}^1 > 1$, condition
11 **H3** indicates that $a\bar{P}^i > 1, 1 \leq i \leq n$. Now define $L(P, H) = H$ as an average Ly-
12apunov function, then we have $L(P, H)|_{S_2} = 0$. Moreover, for the model (3.5)–(3.6),
13 we have

$$14 \quad \sup_{t \geq 0} \liminf_{(P_0, H_0) \rightarrow (\bar{P}^i, 0)} \frac{H_t}{H_0} = \sup_{t \geq 0} \liminf_{(P_0, H_0) \rightarrow (\bar{P}^i, 0)} \left(\prod_{j=0}^{t-1} P_j \frac{1 - e^{aH_j}}{H_j} \right)^t = \sup_{t \geq 0} (a\bar{P}^i)^t > 1$$

15 and for the model (3.7)–(3.8) we have

$$16 \quad \sup_{t \geq 0} \liminf_{(P_0, H_0) \rightarrow (\bar{P}^i, 0)} \frac{H_t}{H_0} = \sup_{t \geq 0} \liminf_{(P_0, H_0) \rightarrow (\bar{P}^i, 0)} \left(\prod_{j=0}^{t-1} F(P_j) \frac{1 - e^{aH_j}}{H_j} \right)^t = \sup_{t \geq 0} (a\bar{P}^i)^t > 1,$$

17 where $(P_0, H_0) \in X_{11}$. Therefore, according to Theorem 2.2 and its Corollary 2.3
18 in [14], we can show that the systems (3.5)–(3.6) and (3.7)–(3.8) are uniformly
19 persistent. Hence, the statement holds. \square

20 **Remark.** The arguments used to prove Theorem 4.5 are standard, which can be
21 found in many literatures (e.g. [12, 17, 19]).

22 5. Application and Simulations

23 5.1. The Beverton–Holt and Holling type III models

24 In this section, we focus on two typical models for the plant dynamics and apply
25 our results:

(1)

$$26 \quad P_{t+1} = F(P_t) = \frac{rP_t}{1 + P_t} \tag{5.1}$$

27 is the Beverton–Holt model, where $F(P_t)$ satisfies the assumptions of **H1** and
28 $f(P_t)$ satisfies those of **H2**. The two equilibria are $\bar{P}^0 = 0$ and $\bar{P}^1 = r - 1$. From
29 Proposition 2.1, we know that \bar{P}^0 is a sink if $r < 1$; \bar{P}^0 is a source if $r > 1$. In
addition, \bar{P}^1 , if it exists, is always a sink.

12 Y. Kang & D. Armbruster

(2) A Holling type III model is given by

$$P_{t+1} = F(P_t) = \frac{rP_t^2}{1 + P_t^2}, \quad (5.2)$$

1 where $F(P_t)$ satisfies **H1**. The equilibria are $\bar{P}^0 = 0$, $\bar{P}^1 = \frac{r - \sqrt{r^2 - 4}}{2}$ and $\bar{P}^2 =$
 2 $\frac{r + \sqrt{r^2 - 4}}{2}$. If $r < 2$, then \bar{P}^0 is the only equilibrium and it is globally stable. If
 3 $r > 2$; \bar{P}^0 is a sink, \bar{P}^1 is a source and \bar{P}^2 is a sink.

4 The plant–herbivore models with (5.1) and (5.2) as plant dynamics become:

5 **Model I:**

(1)

$$P_{t+1} = \frac{rP_t}{1 + P_t} e^{-aH_t}, \quad (5.3)$$

$$H_{t+1} = P_t[1 - e^{-aH_t}], \quad (5.4)$$

(2)

$$P_{t+1} = \frac{rP_t^2}{1 + P_t^2} e^{-aH_t}, \quad (5.5)$$

$$H_{t+1} = P_t[1 - e^{-aH_t}]. \quad (5.6)$$

6 **Model II:**

(1)

$$P_{t+1} = \frac{rP_t}{1 + P_t} e^{-aH_t}, \quad (5.7)$$

$$H_{t+1} = \frac{rP_t}{1 + P_t} [1 - e^{-aH_t}], \quad (5.8)$$

(2)

$$P_{t+1} = \frac{rP_t^2}{1 + P_t^2} e^{-aH_t}, \quad (5.9)$$

$$H_{t+1} = \frac{rP_t^2}{1 + P_t^2} [1 - e^{-aH_t}]. \quad (5.10)$$

7 Applying the results of the previous section, we have the following two corollaries.

8 **Corollary 5.1.** *The three models (5.3)–(5.4), (5.7)–(5.8) and (5.9)–(5.10) have at*
 9 *most one interior equilibrium. The interior equilibria of Model I (5.3)–(5.4) and*
 10 *Model II (5.7)–(5.8) emerge through a transcritical bifurcations from the boundary*
 11 *equilibrium $(\bar{P}^1, 0) = (r - 1, 0)$ when $a(r - 1) = 1$ and $r > 1$; the interior equilib-*
 12 *rium of Model II (5.9)–(5.10) emerges through a transcritical bifurcations from the*
 13 *boundary equilibrium $(\bar{P}^2, 0) = (\frac{r + \sqrt{r^2 - 4}}{2}, 0)$ when $a\frac{r + \sqrt{r^2 - 4}}{2} = 1$ and $r > 2$.*

1 **Corollary 5.2.** *If $a(r - 1) > 1$, the systems (5.3)–(5.4) and (5.7)–(5.8) are*
 2 *uniformly persistent with respect to $(X_{11}, \partial X_{11})$.*

3 **5.2. Periodic orbits and heteroclinic bifurcations**

4 The stability of the single interior equilibrium of models (5.3) to (5.10) depends on
 5 the values of the parameters r and a . As the values of r or a increase, the interior
 6 equilibrium goes through a Neimark–Sacker bifurcation generating an invariant
 7 cycle.

8 Since Models I and II have similar dynamics, we only focus on Model II and
 9 discuss the Beverton–Holt model (5.1) and the Holling type III model (5.2), respec-
 10 tively. The main difference between the Beverton–Holt model and the Holling type
 11 III model is that the Holling type III model can show a heteroclinic bifurcation
 12 where a periodic orbit grows until it becomes a heteroclinic connection between
 13 boundary equilibria whereas the Beverton–Holt model does not show such a bifur-
 14 cation. Figure 2 shows the heteroclinic bifurcation schematically: when $a = 0.71$
 15 and $r = 2.5$, the system has a stable interior equilibrium (the dark dot that is in the
 16 middle of the figure, which is generated by the Matlab); when we increase r to 3.5
 17 and keep $a = 0.71$, the system has an invariant orbit (the grey orbit in the figure,
 18 which is generated by the Matlab); however, if we continue to increase the values
 19 of a or r , the invariant orbit disappears and the system converges to the boundary
 20 equilibrium $(0, 0)$. This suggests that a heteroclinic bifurcation occurs (the dark
 21 line with arrows in the figure, which is generated schematically).

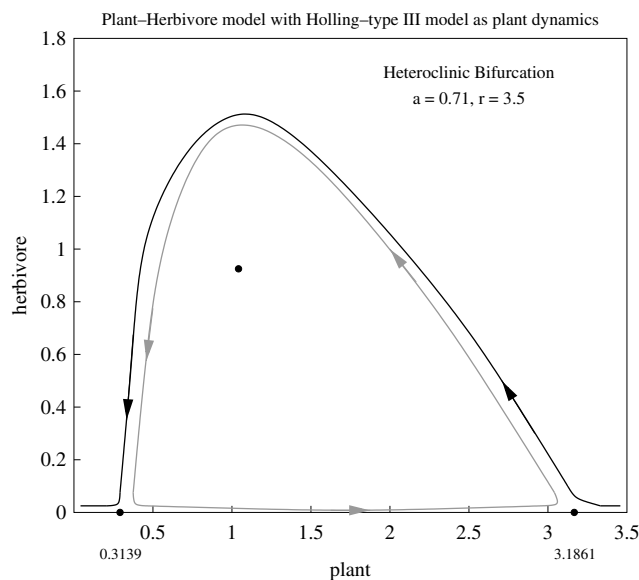


Fig. 2. Schematic of the heteroclinic bifurcation of Holling type III model happens at $a = 0.71, r = 3.5$.

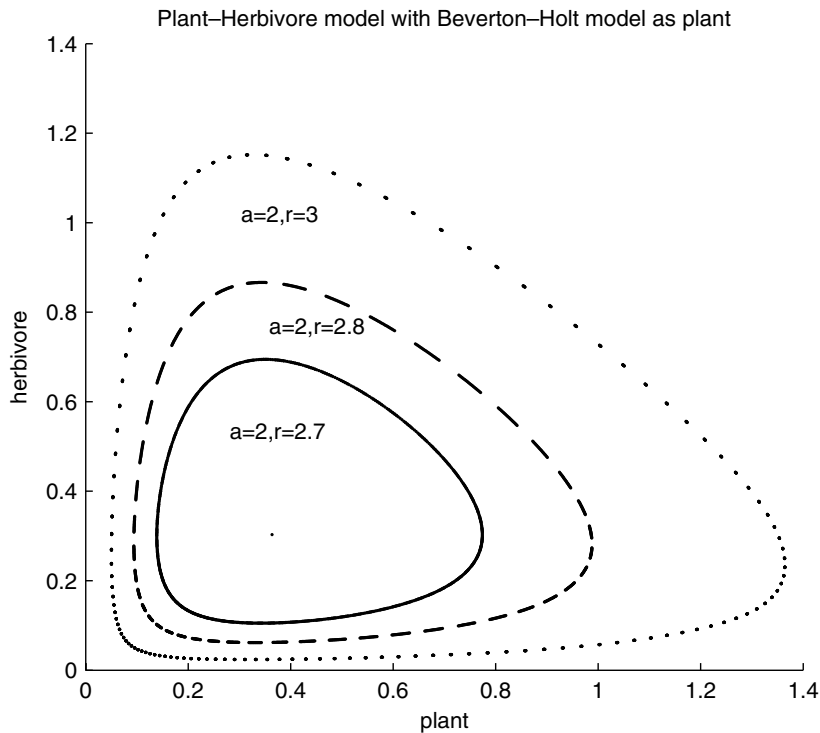
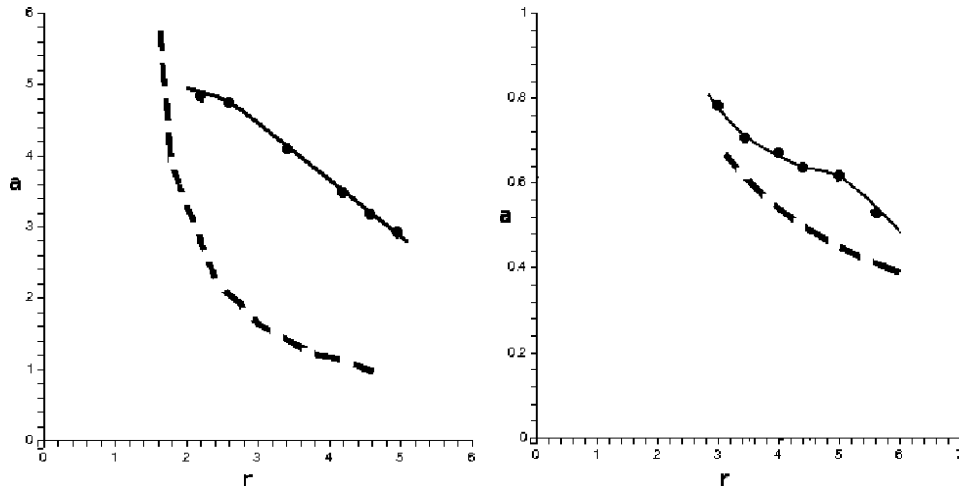


Fig. 3. The periodic orbit for the Beverton–Holt model when $a = 2$, $r = 2.5, 2.7, 2.8, 3$.

1 Since the Beverton–Holt model only has the origin as a saddle and one other
 2 boundary equilibrium and since the stable manifold of the origin is the H -axis which
 3 is an invariant manifold, the periodic orbit in the interior cannot become hetero-
 4 clinic. However, it can become very large and pass the origin arbitrarily close to the
 5 coordinate axes as shown in Fig. 3. Figure 3 is the numerical simulations generated
 6 by the Matlab for 2000 generations when $a = 2$ and $r = 2.5, 2.7, 2.8, 3$. When $a = 2$
 7 and $r = 2.5$, the system has a stable interior equilibrium as shown in the figure
 8 (small dark dot); when $r = 2.7, 2.8, 3$, the system has an invariant orbit. Numerical
 9 simulations of this case hint at an interesting phenomenon: a standard numerical
 10 simulation shows the periodic orbit disappearing and the trajectory approaching
 11 the non-trivial boundary equilibrium as time increases. However, that boundary
 12 equilibrium is a saddle and the trajectory should leave into the interior but it does
 13 not do so over any simulation time that we checked. The resolution of the puzzle
 14 comes from the considerations of the accuracy of the simulations: as the limit cycle
 15 gets closer to the origin, the herbivore values become so small that they are approx-
 16 imated as zero. Hence the dynamics is reduced to the dynamics of the plant which
 17 has a stable equilibrium on the invariant manifold determined by $H = 0$ and hence
 18 the trajectory never leaves.



(a) The bifurcation diagram for the Beverton–Holt model.

(b) The bifurcation diagram for the Holling type III model.

Fig. 4. The Neimark–Sacker bifurcation and heteroclinic bifurcations.

1 Figure 4(a) shows a “bifurcation diagram” for the Beverton–Holt model, which
 2 describes the Neimark–Sacker bifurcation curve (dashed line) and the “collapse
 3 curve” (solid line). The latter represents an interpolation of numerical simulations
 4 with a and r values for which a standard Matlab numerical precision simulation does
 5 not detect a population of the herbivore. Figure 4(b) is a bifurcation diagram for
 6 a Holling type III model showing interpolations of the Neimark–Sacker bifurcation
 7 curve (dashed line) and the heteroclinic bifurcation (solid line), respectively.

8 5.3. Noise-generated outbreaks

9 The extreme sensitivity of the periodic orbit in the Beverton–Holt model suggests
 10 that noise may play a much bigger role than previously discussed in the outbreaks
 11 of herbivore infestations. Once the periodic orbit disappears due to accuracy issues,
 12 we can make it re-appear by adding small amount of noise to the simulation:

- 13 (1) *Noise*: We use positive white noise to make sure the system stays positive, i.e.
 14 we sample from a normal distribution but discard any negative noise sample.
- (2) *Population of herbivores*: For each generation, we add the noise to the
 herbivore, i.e.

$$H_{t+1} = \frac{rP_t e^{-aH_t}}{1 + P_t} + \omega R_n, \quad (5.11)$$

15 where R_n is a positive white noise as defined above and ω is the amplitude of
 16 the noise. See Fig. 5, for example, in this case, the amplitude of the positive
 17 white noise is $\omega = 0.01$.

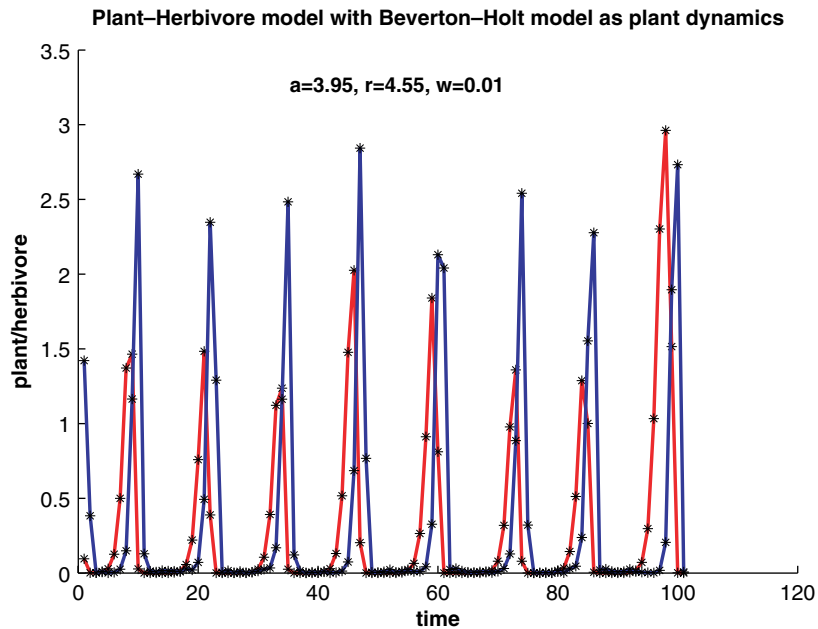


Fig. 5. Time series of the herbivore population for the Beverton–Holt model. The parameters are $a = 3.95, r = 4.55$ and a noise level of $w = 0.01$.

1 At that time the trajectories look like a randomly occurring bursting phenomenon
 2 that nevertheless has a well-defined average periodicity (see Fig. 5). Given by the
 3 exact nature of the model there will be a *threshold* at which the population of the
 4 herbivore cannot be detected in nature. We define the *resident time* as the time
 5 interval for which the population of the herbivore stays below some threshold, e.g.
 6 0.01 and the *resident time ratio* as the ratio of the residence time to the period of
 7 the bursting. Table 2 shows the period as a function of the mean square amplitude
 8 of the noise level. Figure 6 shows the resident time ratio as a function of the noise
 9 amplitudes. The figure is generated by calculating the resident time ratio for each
 10 noise amplitude for 50 trajectory with 1000 generations. Figure 6 shows that over
 11 many orders of magnitude the residence ratio stays around 80% indicating that the
 12 herbivore is dormant for most of the time and only appears for about 20% of its
 13 periodic cycle. Table 2 indicates that by choosing a particular noise level, we can
 14 control the apparent periodicity of the bursts.

15 In particular, time intervals of the herbivore outbreaks around 8–12 years can
 16 be generated, which fits the ecological data for gypsy moth outbreaks [22]. Also, for

Table 2. Average period of the herbivore dynamics when $a = 3.95, r = 4.55$.

Amplitude of noise w	0.01	0.001	0.0001	0.00001	0.000001	0.0000001
Period t	8	10	12	14	17	19

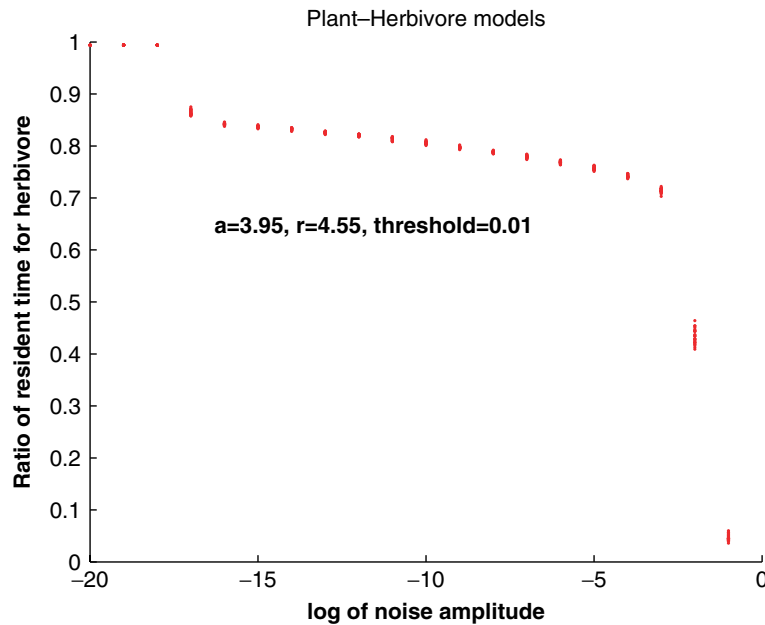


Fig. 6. The resident time ratio as a function of the noise amplitude when $a = 3.95$, $r = 4.55$ with a threshold of 0.01.

1 larger noise levels, the distribution of the periods is rather broad, which also seems
 2 to be happening for real data (see [18, 25]).

3 6. Conclusions and Additional Features

4 For most plant species, it is conceivable that there is density-dependent regulation
 5 of its growth. However, very few plants show periodic or strongly chaotic variation of
 6 the plant density from generation to generation. Hence it is important to determine
 7 the influence of models of monotone growth dynamics on the plant–herbivore inter-
 8 action model. We proved three key features of such interactions that are important
 9 for model building:

- 10 • All monotone growth models generate a unique interior equilibrium.
- 11 • Monotone growth models with just one sustainable equilibrium for the plant
 12 population (e.g. the Beverton–Holt model) lead to noise sensitive bursting. This
 13 certainly happens for many plant–herbivore systems and the dynamical mech-
 14 anism discussed here has not been noticed before in plant–herbivore systems
 15 (however, see [25]).
- 16 • Models I and II have a uniformly persistent property if they satisfy both **H1**
 17 and **H3**. In particular, the Beverton–Holt model is uniformly persistent and the
 18 Holling type III model is not.

18 Y. Kang & D. Armbruster

- 1 • The Beverton–Holt model does not have more complicated dynamics than a
 2 periodic orbit in the interior of the phase space. Although we cannot prove this,
 3 we conjecture that this is true for all models that satisfy the assumptions of **H1**
 4 and **H2**, i.e. have just one equilibrium for the pure plant dynamics.

5 Without any claim to a complete analysis of all types of models, we note a few addi-
 6 tional features associated with monotone and non-monotone plant growth models.

- 7 (1) *Bistability*: The paper [16] study plant–herbivore systems of Model II type
 8 with a Ricker model for the pure plant dynamics, also known as the modified
 9 Nicholson–Bailey model. It is shown that for a large set of parameters the
 10 system exhibits bistability between complicated (possibly chaotic) dynamics
 11 in the interior of the phase space and equally complicated dynamics on the
 12 boundary (Fig. 7). Kon [20] discusses a similar bistability phenomenon for
 13 Model I. Since unimodal maps are all topologically equivalent [9], we expect
 14 bistability to be a defining feature for plant–herbivore models with unimodal
 15 plant growth models.

16 In contrast, models that satisfy the assumptions of **H1** and **H3**, e.g. the
 17 Beverton–Holt model cannot show bistability since the global attractor either
 18 is a fixed point on the boundary or some set in the interior of the phase space.
 19 However, it is conceivable that models that do not satisfy **H3**, e.g. Holling

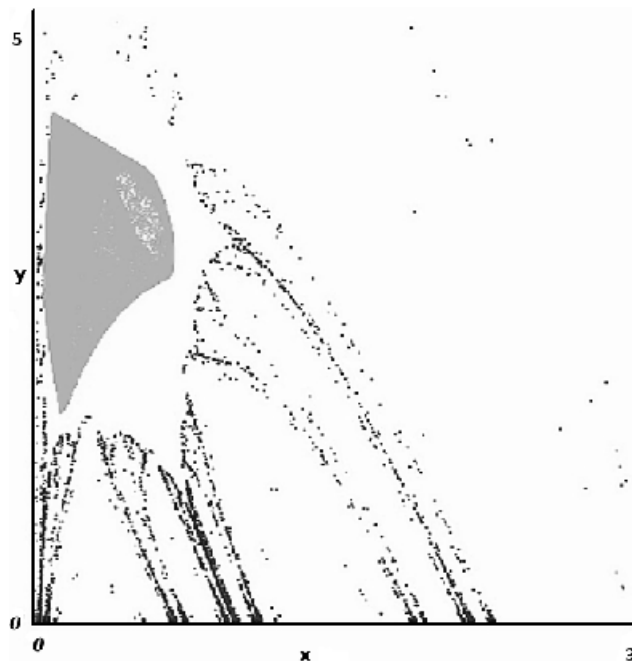


Fig. 7. The interior strange attractor and the stable manifold of the boundary attractor $a = 0.95, r = 3.8$.

- 1 type III models, show bistability between an interior attractor and a boundary
 2 equilibrium that is not the largest equilibrium for the pure plant population.
- 3 (2) *Crises of Interior Attractors*: All models seem to show some sort of global
 4 attraction to the boundary dynamics, i.e. extinction of the parasite for large
 5 growth rates r :
- 6 • Unimodal models show a crisis type of bifurcation whereas the chaotic
 7 dynamics in the interior collapses and the system becomes globally attracted
 8 to the boundary dynamics [16]. For instance, the interior strange attractor
 9 in Fig. 7 that exists for a growth parameter of $r = 3.8$ will grow and hit the
 10 stable manifold of the boundary attractor for $r = 3.85$.
 - 11 • Holling type III models show a heteroclinic orbit which breaks and leads to
 12 global attraction to a boundary fixed point.
 - 13 • *Conjecture*: The Beverton–Holt model does not lead to complete extinction
 14 according to Theorem 4.5. However, ϵ in Theorem 4.5 may happen to be
 15 small which, taking a stochastic effect into account, might lead to extinction
 16 of herbivores.

17 Acknowledgments

18 The research of D.A. is supported by NSF grant DMS-0604986. The authors would
 19 like to thank the anonymous referees for comments that helped to improve the
 20 paper. We also thank Nicolas Lanchier for his help producing some of the figures.

21 References

- 22 [1] K. C. Abbott and G. Dwyer, Food limitation and insect outbreaks: Complex dynam-
 23 ics in plant–herbivore models, *J. Animal Ecol.* **76** (2007) 1004–1014.
- 24 [2] J. R. Beddington, C. A. Free and J. H. Lawton, Dynamic complexity in predator–prey
 25 models framed in difference equations, *Nature (London)* **225** (1975) 58–60.
- 26 [3] R. J. H. Beverton and S. J. Holt, On the dynamics of exploited, *Fish Populations*
 27 Gt. Britain, Fishery Invest., Ser. **II**, Vol. **XIX**, 533.
- 28 [4] J. E. Cohen, Unexpected dominance of high frequencies in chaotic nonlinear popu-
 29 lation models, *Nature* **378** (1995) 610–612.
- 30 [5] M. J. Crawley, *Herbivory: The Dynamics of Animal–Plant Interactions*, Studies in
 31 Ecology, Vol. 10 (University of California Press, 1983).
- 32 [6] M. J. Crawley and G. J. S. Ross, The population dynamics of plants [and discussion],
 33 *Philos. Trans. Biol. Sci.* **330**(1257) (1990) 125–140.
- 34 [7] J. M. Cushing and S. M. Henson, Global dynamics of some periodically forced, mono-
 35 tone difference equations, *J. Difference Eqs. Appl.* **7** (2001) 859–872.
- 36 [8] T. Dhirasakdanon, A model of disease in amphibians, Ph.D. thesis, Arizona State
 37 University (2010).
- 38 [9] J. Guckenheimer, Sensitive dependence on initial conditions for unimodal maps,
 39 *Commun. Math. Phys.* **70** (1979) 133–160.
- 40 [10] J. L. Harper, *Population Biology of Plants* (Academic Press, New York, 1977),
 41 pp. 1035–1039.
- 42 [11] S. M. Henson and J. Cushing, Hierarchical models of intra-specific competition:
 43 Scramble versus contest, *J. Math. Biol.* **34** (1996) 1416–1432.

- 1 [12] J. Hofbauer, V. Hutson and W. Jansen, Coexistence for systems governed by differ-
2 ence equations of Lotka–Volterra type, *J. Math. Biol.* **25** (1987) 553–570.
- 3 [13] J. Hofbauer and J. W.-H. So, Uniform persistence and repellers for maps,
4 *Proc. Amer. Math. Soc.* **107** (1989) 1137–1142.
- 5 [14] V. Hutson, A theorem on average Liapunov functions, *Monatsh. Math.* **98** (1984)
6 267–275.
- 7 [15] S. R.-J. Jang, Allee effects in a discrete-time host-parasitoid model, *J. Difference*
8 *Eqs. Appl.* **12** (2006) 165–181.
- 9 [16] Y. Kang, D. Armbruster and Y. Kuang, Dynamics of a plant–herbivore model,
10 *J. Biol. Dynamics* **2**(2) (2008) 89–101.
- 11 [17] Y. Kang and P. Chesson, Relative nonlinearity and permanence, *Theor. Popul. Biol.*
12 **78** (2010) 26–35.
- 13 [18] B. E. Kendall, C. J. Briggs and W. W. Murdoch, Why do populations cycle? A synthe-
14 sis of statistical and mechanistic modeling approaches, *Ecology* **80** (1999) 1789–1805.
- 15 [19] R. Kon, Permanence of discrete-time Kolmogorov systems for two species and satu-
16 rated fixed points, *J. Math. Biol.* **48** (2004) 57–81.
- 17 [20] R. Kon, Multiple attractors in host-parasitoid interactions: Coexistence and extinc-
18 tion, *Math. Biosci.* **201**(1–2) (2006) 172–183.
- 19 [21] R. Law and A. R. Watkinson, Response-surface analysis of two-species competition:
20 An experiment on phleum arenarium and vulpia fasciculata, *J. Ecol.* **75**(3) (1987)
21 871–886.
- 22 [22] A. M. Liebhold, N. Kamata and T. Jacob, Cyclicity and synchrony of historical
23 outbreaks of the beech caterpillar, *Quadricalcarifera punctatella* (Motschulsky) in
24 Japan, *Res. Popul. Ecol.* **38**(1) (1996) 87–94.
- 25 [23] L. A. Real, The kinetics of functional response, *Amer. Nat.* **111** (1977) 289–300.
- 26 [24] W. E. Ricker, Stock and recruitment, *J. Fish. Res. Board Can.* **11** (1954) 559–623.
- 27 [25] S. Rinaldi, M. Candaten and R. Casagrandi, Evidence of peak-to-peak dynamics in
28 ecology, *Ecol. Lett.* **4**(6) (2001).
- 29 [26] L.-I. W. Roeger, Dynamically consistent discrete-time Lotka–Volterra competition
30 models, accepted.
- 31 [27] P. L. Salceanu, Lyapunov exponents and persistence in dynamical systems, with
32 applications to some discrete-time models, Ph.D. thesis, Arizona State University
33 (2009).
- 34 [28] H. L. Smith and H. R. Thieme, Dynamical systems and population persistence, in
35 preparation.
- 36 [29] J. Smoller, *Shock Waves and Reaction–Diffusion Equations*, 2nd edn. (Springer-
37 Verlag, New York, 1994).
- 38 [30] S. Tang and L. Chen, Chaos in functional response host-parasitoid ecosystem models,
39 *Chaos, Solitons Fractals* **13** (2002) 875–884.
- 40 [31] M. Tuda and Y. Iwasa, Evolution of contest competition and its effect on host-
41 parasitoid dynamics, *Evol. Ecol.* **12** (1998) 855–870.
- 42 [32] A. R. Watkinson, Density-dependence in single-species populations of plants,
43 *J. Theor. Biol.* **83** (1980) 345–357.